HHS Public Access

Author manuscript

Nat Methods. Author manuscript; available in PMC 2012 January 04.

Published in final edited form as:

Nat Methods. 2009 February ; 6(2): 147–152. doi:10.1038/nmeth.1290.

Microfluidic Control of Cell Pairing and Fusion

Alison M. Skelley[1,2,¶], **Oktay Kirak**[3,¶], **Heikyung Suh**[3], **Rudolf Jaenisch**[3,4], and **Joel Voldman**[1,2,5]

[1]Research Laboratory of Electronics, 50 Vassar Street, Massachusetts Institute of Technology, Cambridge, MA 02139

[2]Microsystems Technology Laboratory, 60 Vassar Street, Massachusetts Institute of Technology, Cambridge, MA 02139

[3]Whitehead Institute for Biomedical Research, Nine Cambridge Center, Cambridge, MA 02142

[4]Department of Biology, Massachusetts Institute of Technology, 77 Massachusetts Avenue, Cambridge, Massachusetts 02139

[5]Electrical Engineering and Computer Science Department, 77 Massachusetts Avenue, Massachusetts Institute of Technology, Cambridge, MA 02139

Abstract

Cell fusion has been used for many different purposes, including generation of hybridomas and reprogramming of somatic cells. The fusion step represents the key event in initiation of these procedures. Standard fusion techniques, however, provide poor and random cell contact, leading to low yields. We present here a microfluidic device to trap and properly pair thousands of cells. Using this device we were able to pair different cell types, including fibroblasts, mouse embryonic stem cells (mESCs), and myeloma cells, achieving pairing efficiencies up to 70%. The device is compatible with both chemical and electrical fusion protocols. We observed that electrical fusion was more efficient than chemical fusion, with membrane reorganization efficiencies of up to 89%. We achieved greater than 50% properly paired and fused cells over the entire device, 5× greater than a commercial electrofusion chamber, and were able to observe reprogramming in hybrids between mESCs and mouse embryonic fibroblasts.

Corresponding Authors: Joel Voldman, voldman@mit.edu, Department of Electrical Engineering & Computer Science, Massachusetts Institute of Technology, Room 36-824, 77 Massachusetts Ave, Cambridge, MA 02139, Ph: 617.253.2094, Fx: 617.258.5846. Rudolf Jaenisch, jaenisch@wi.mit.edu, Member, Whitehead Institute for Biomedical Research, Professor of Biology, Massachusetts Institute of Technology, Nine Cambridge Center, Cambridge, Massachusetts 02147-1479, Ph: 617.258.5186, Fx: 617.258.6505.

¶These authors contributed equally to this work.

Author Contributions:

A.M.S. designed, performed and analyzed experiments, and drafted the manuscript. O.K. designed, performed and analyzed experiments, and drafted the manuscript. H.S. generated the GFP-positive cells and mice and performed experiments. R.J. participated in experimental design, analyzed data and drafted the manuscript. J.V. participated in experimental design, analyzed data and drafted the manuscript.

Introduction

Fusion provides a unique tool to combine genetic and epigenetic information of two different cells. Since its first application in the 1960s, it has been mainly used to identify trans-acting factors that affect gene expression as well as to generate antibody-producing hybridomas[1–3]. More recently, the fusion of enucleated oocytes and embryonic germ cells (EGC) with somatic cells has provided definitive evidence for epigenetic reprogramming mediated via trans-acting factors[4,5]. Besides EG cells, embryonic stem cells (ESC), and embryonic carcinoma cells (ECC) also have been proven to reprogram somatic cells[3,6–8]. In all of these cases, fusion is the crucial step, but technical limitations in how fusion is carried out have prevented detailed studies of fusion-mediated reprogramming. As a result, the mechanisms by which the transcriptional program of a cell is altered after fusion, leading to nuclear reprogramming, remains largely unknown.

Fusion of cells can be induced biologically (viruses, receptors)[2,9], chemically (Polyethylene Glycol)[10,11], or physically (electric pulse)[12,13], with the latter two representing the two most commonly used techniques. Both chemical and electrical fusion rely on random cell-cell pairing and result in low overall fusion efficiencies, requiring antibiotic selection and lengthy subculturing to isolate the desired hybrids. Alternatively, single cells can be manually immobilized and then paired[14], resulting in precise fusion partners, but low numbers of fused cells.

Improving the process of cell fusion lies in both the mechanism of initiating membrane fusion as well as in controlling how the cells are brought into contact and properly paired. There have been previous attempts using microfluidics for cell pairing, utilizing either flow-through or immobilization techniques to improve cell contact. Flow-through approaches, in which cells are brought into contact through AC fields or biotin-streptavidin coatings, demonstrate that higher membrane fusion efficiencies can be achieved[15–18]. However, these approaches lack the ability to properly pair and fuse unmodified cells, and the overall yield of desired fusions remains low. Immobilization techniques using hydrodynamic weirs or suction have demonstrated the ability to properly pair cells, and these devices have been used successfully for electroporation[19–23], but thus far are incapable of pairing and fusing cells.

Here we present a microfluidic device containing a dense array of weir-based passive hydrodynamic cell traps. Using a novel geometry and a 3-step loading protocol, we can immobilize and pair thousands of cells at once. The device is compatible with both chemical and electrical fusion protocols. We demonstrate the utility of our device for pairing and fusing different cell types, including NIH3T3 fibroblasts, myeloma cells, B cells, mESCs and mouse embryonic fibroblasts (mEFs), improving fusion efficiencies to > 50%. Further, our device allows observation of fusions on-chip without losing registration within the array, enabling us to identify and analyze properly fused cells. Finally, we demonstrate that NIH3T3-NIH3T3 as well as mESC-mEF hybrids can be cultured for prolonged time after fusion in our device and are able to reprogram mouse embryonic fibroblasts after fusion to embryonic stem cells.

Results

Microfluidic Device Design

The cell capture device is comprised of thousands of polydimethyl siloxane (PDMS) cell traps densely arrayed within a flow-through channel. Each cell trap consists of a weir structure that extends vertically into the channel and contains front- and backside capture cups (Fig. 1a–d). Support pillars placed on either side of the capture cups allow flow into and under the trap. We tailored the pillar heights to be slightly smaller than the cell diameter so the cells were trapped once they entered the capture cup. The support pillars also maintained proper channel height across the array once the device was bonded to a glass substrate. The cell traps were incorporated into three different devices; the largest was 8 mm × 4 mm and contained ~6000 traps (Fig. 1e). We observed that the trap spacing within the array was critical for efficient capture without clogging. With optimal column spacing (~1–1.5 cell diameters, ~20 μm) and a row spacing of 20 to 50 μm we could capture 70–90% of the cells that entered the array (Supplementary Fig. 1).

Cell Capture and Pairing

We accomplished two-cell capture and pairing using a 3-step loading protocol. We first isolated single cells in the smaller backside capture cup (Fig. 2a). Once the array was saturated, the cells were transferred directly “down” into the opposing larger capture cup (Fig. 2b). This transfer was fast (< 1s), massively parallel and highly efficient because of the laminar flow within the device (Supplementary Video 1 online). Finally, the second cell population was loaded and trapped immediately in front of the previously trapped cells (Fig. 2c). The larger frontside cup was sized to trap two cells, so additional cells traveled through the array until it was saturated. We obtained two-cell capture efficiencies up to ~80% (percentage of traps occupied by exactly 2 cells of any type), and pairing efficiencies of up to 70% (Fig. 2d, see also Supplementary Discussion online). Higher efficiencies were possible in the middle and bottom of the array where less penetration of larger cell clumps and therefore better single cell transfer occurred.

Fusion in the Microfluidic Device

We next aimed to test the compatibility of our device with both chemical and electrical fusion protocols. We determined fusion efficiencies by imaging and quantifying both the exchange of fluorescent proteins (indicative of initiation of fusion) and plasma membrane reorganization (indicative of advanced fusion). In some experiments we determined complete fusion after prolonged culture *in vitro*. We paired and fused different cell types, including NIH3T3 fibroblasts, mESCs, mEFs, B cells and myeloma cells

We first explored the capability of our device to fuse cells using PEG. We flowed PEG past the cells[please specify which cells were used in video 2], causing them to shrink from the osmotic shock (Supplementary Video 2 online). During this time the cells remained in contact and stationary within the array, demonstrating that our trap geometry can successfully immobilize the cells even though there is a substantial change in cell volume. Next, we washed the PEG out with media, causing the cells to swell back to their original size and initiate fusion. An advantage of our device is that solutions can be exchanged

rapidly while the cells remain paired and in contact; therefore further doses of PEG can be applied to increase fusion efficiencies without losing cell pairing or registration. A single dose of PEG yielded 15% fluorescence exchange over CellTracker-stained 3T3 pairs and 8% membrane fusion of unstained 3T3 cells, while subsequent doses of PEG yielded up to 35% fluorescence exchange over red/green pairs and 25% membrane reorganization of unstained 3T3 cells (Supplementary Fig. 2 and Supplementary Video 3 online). Viability staining with trypan blue indicated an increase in cell death with additional doses of PEG, eventually limiting the effectiveness of subsequent doses.

We then adapted our device to be compatible with electrofusion protocols. In order to introduce electric fields we plasma-bonded the device to a glass slide containing metal electrodes (Fig. 1e). Once the cells [please specify the cells in video 4]were paired and immobilized, we flowed hypoosmolar fusion buffer past the cells, causing the cells to swell. The capture cups utilized were slightly deeper to accommodate the cells as they got larger (Supplementary Video 4 online). Again, as with the PEG protocol, the cells remained immobilized and paired as they changed size. An added benefit is that the cells are pre-aligned and in contact so no AC field is required. We analyzed membrane fusion after the electrical pulse (Supplementary Videos 4, 5 and Supplementary Fig. 3 online). We found electrofusion to be significantly more efficient than PEG ($P < 0.05$); a single series of pulses yielded 78% fluorescence exchange over CellTracker red/green pairs and 89% membrane reorganization of unstained 3T3 cells.

Characterization of Cell Fusion

Another advantage of our device is the ability to observe the progression of fusion at the single-cell level. Before and immediately after the PEG application two distinct membranes were visible and fluorescence was still localized within each cell (Fig. 3a). After 10 minutes green fluorescence was observed within the mEF demonstrating that the cytosols of the two cells had connected and fusion was initiated. The Hoechst fluorescence was still localized in the mEF, indicating that the nucleus was intact. After 15 min the plasma membranes began to reorganize, leading to a hybrid cell containing the contents of both cells. The Hoechst fluorescence remained partitioned in the new hybrid cell, suggesting no nuclear fusion had taken place. Electrofusion followed a different timecourse (Fig. 3b–c). Interestingly, fluorescence exchange was detected within seconds after the electric pulse, and in most cases the outline of the nucleus was visible as the fluorescence first moved into the cytoplasm. This exchange of fluorescence was clear even though the cell membranes had yet to reorganize. After 10–20 min the plasma membranes began to reorganize. By immobilizing the cells we were able to observe and distinguish between the exchange of cell contents and membrane reorganization for single pairs.

Quantification of Fusion over the Array

Immobilizing the cells in a dense array also provides the opportunity to observe fusion for thousands of cell pairs in parallel. We used computational image analysis to monitor fluorescence exchange over the entire device in a fashion similar to a FACS plot (Supplementary Figs. 4–6 online). Immediately after the electrical pulse the red-green double-positive population increased to 53.5%. With increasing time more cells exchanged

fluorescence (maximum 63.9% at t = 5 min). In addition, the amount of fluorescence exchanged also increased as shown by the red-green double-positive cell populations moving towards the center of the plot. This indicates that connections are established which allow continual exchange and eventual equilibration of cytosolic material[24]. Slight decreases at later times were artifacts due to cells shrinking and moving out of the range of the analysis box.

Comparison of PEG fusion with Electrofusion

Our device allows direct comparison of the fusion efficiencies of different fusion stimuli. We compared PEG and electrofusion efficiencies of properly paired cells determined by manually inspecting the images and evaluating the fluorescence exchange or membrane reorganization (Fig. 4a). Since this measurement is independent of the capture and pairing efficiency, it provides a comparison of different fusion techniques. Using PEG, we were able to initiate fusion of 39% ± 14% of cell pairs, while electrofusion resulted in a significantly higher 78 ± 12% fusion pairs ($P < 0.05$). These electrofusion efficiencies were comparable to those obtained when *Discosoma sp.* red fluorescent protein (DsRed)-expressing and enhanced green fluorescent protein (eGFP)-expressing cells were fused electrically in the device (68 ± 24%, with a single-run high of 91%), and with CellTracker-stained mESCs and mEFs (single-run value of 56%). We also placed cells in the device and cultured for three days without fusion stimulus (Supplementary Fig. 7 online); no doubly labeled cells were observed, indicating that negligible fusion occurred in the absence of fusogenic stimuli.

Comparison to Standard Macroscale Fusion Protocols

We compared the overall efficiencies in generating fused cells with our device to standard commercial PEG and electrofusion instruments and protocols. To compare between commercial and chip-based protocols, we primarily used a common fusion metric of fluorescence exchange that could be assessed for all protocols and has been used by others[25,26], and used membrane re-organization for the on-chip PEG experiments. Fluorescence exchange (% red-green double-positive cells over the whole cell population) was determined either by our image analysis program or by FACS while membrane re-organization was evaluated visually. A standard PEG protocol yielded 6 ± 4% fused cells using stained 3T3 fibroblasts compared with a significantly higher 25 ± 5% obtained after 4 doses of PEG in our microfluidic device ($P < 0.05$, Fig. 4b). When we compared electrofusion performance in a commercial system to the microfluidic device, we found significantly higher fusion efficiencies in the microfluidic device ($P < 0.05$). For stained 3T3 fibroblasts, we obtained 11 ± 9% fusion in the commercial Helix chamber (Eppendorf, Westbury, NY) as compared to 51 ± 16% obtained in our device, while for fluorescent-protein expressing fibroblasts, we obtained 4 ± 2% fused cells in the commercial electrofusion system and 40 ± 13% in the microfluidic device. Finally, we obtained 11 ± 4% electrofusion of stained mESCs and mEFs while 23% was achieved with our device (single run). In all cases the microfluidic device delivered a 2- to 10-fold improvement on fusion yield compared to commercial systems.

Demonstration of Functionality of Fused Cells

We next examined whether cells can be removed from the chip after fusion and can survive prolonged culture. We removed NIH3T3 fibroblasts after fusion in our device (Supplementary Fig. 8 online) and cultured them for 10 days. We obtained viable fused cells as demonstrated by the presence of red-green double-positive cells (Fig. 5a–b), and via FACS analysis (not shown).

Fusions of embryonic stem cells with somatic cells have been used to demonstrate the capability of ES cells to reprogram somatic cells[6,7]. To show that our microfluidic device can also generate viable hybrids between mESCs and mEFs, we fused Hygromycin-resistant mESCs with Puromycin-resistant mEFs in our device and cultured them under self-renewing conditions. After 14 days under double-selection, we observed drug resistant colonies that had an ESC-like morphology and stained positive for alkaline phosphatase (Fig. 5c). Reactivation of embryonic genes, such as Nanog and Oct4, has been used to demonstrate successful reprogramming of somatic cells[7,27,28]. The Puromycin-resistant mEFs carried an additional Oct4-GFP reporter in their endogenous *oct4*-locus, allowing us to investigate whether reprogramming as judged by the reactivation of Oct4-GFP would also occur. We were able to detect alkaline phosphatase-positive colonies that also expressed GFP, demonstrating that our device is suitable for generating viable hybrids and observing reprogramming of mEFs after fusion with mESCs (Fig. 5d).

Discussion

Reprogramming of somatic cells via fusion with ES cells and generation of antibody-producing hybridomas are two applications for *in vitro* cell fusion. An enduring problem is the low-efficiency of generating properly fused cells. High-yield fusion relies on both proper cell pairing and efficient initiation of fusion. As these events are independent of each other, standard fusion techniques, based on random and non-uniform cell contact, lead to low fusion rates. Here, we present a new device for massively parallel cell capture, pairing, fusion and analysis.

Our device was evaluated both on the ability to initiate fusion of cells using different fusion impulses and on the overall efficiency of generating properly fused cells relative to conventional protocols. By controlling for the cell contact and pairing in our device we evaluated the efficiency of different fusion impulses based on independent measurements of fluorescence exchange (initiation of fusion) and membrane reorganization (advanced fusion). Analyzing only the properly paired red and green cells allowed a direct comparison of chemical versus electrical fusion. We observed that electrofusion resulted in higher fusion efficiency as assessed both via fluorescence exchange and membrane fusion, likely due to the tight membrane contact between cell pairs when fused in the cell trap. Although we observed higher fusion efficiencies with electrofusion, this situation may change for cell pairs of widely divergent sizes. Since the threshold voltage for generating pores required for electrofusion depends on cell size, and applying too much voltage across the membrane can cause cell lysis, two cells of very different sizes may be difficult to electrofuse successfully. In this case, PEG fusion may be superior (see also Supplemental Discussion online).

Considering that fusion efficiency depends on both pairing and initiation of fusion, and electrofusion yields in our device are up to ~90%, it is clear that pairing represents the crucial step for high-yield generation of properly fused cells. The 70% pairing efficiency that we are able to achieve is a substantial improvement over the 25% pairing efficiency previously reported for biotin-streptavidin linked cells while not requiring any cell surface modification[17], while the 51% ± 16% fusion efficiency for NIH3T3s represents a 5-fold increase over the control and previously reported microfluidic fusion yields[17,18].

Additionally, the design of our microfluidic device allowed us to study cytoplasmic exchange for thousands of fusion events in parallel. Interestingly, we observed a slower mode of membrane reorganization in cells stained with CellTracker dyes. For example, 25 min after fusion initiation, 24% of CellTracker-stained 3T3 fibroblasts had reorganized membranes versus 91% of eGFP/DsRed-expressing 3T3 fibroblasts. Close inspection indicated that for many CellTracker-stained cells the fluorescence was still somewhat partitioned and the membrane reorganization, though initiated, was not completed within the same time frame as for as eGFP/DsRed-expressing cells (Supplementary Fig. 9).

As commercial fusion techniques have low efficiency but can still generate viable hybrids using both PEG and electric fusion, we sought to demonstrate that our microfluidic device is also able to generate viable hybrids. We performed long-term culture of fused fibroblasts and demonstrated that fused mESC-mEF hybrids could adopt an ESC-like morphology, stain for alkaline phosphatase and, most importantly, showed evidence of reprogramming as judged by reactivation of an endogenous Oct4-GFP reporter (Fig. 5).

In conclusion, we present a PDMS-based device to allow highly efficient pairing of different cell types. We were able to achieve > 50% of properly paired and fused cells, enabling the use of these cells for future pooled population assays. Our device provided insight into the fusion process, allowing us to decouple fluorescence exchange and membrane reorganization and to compare PEG and electric fusion. The device can be used for on-chip analysis of a variety of fusion-based studies between 2-color, 1-color and even unstained cells. In addition, cells fused within our device maintained their viability and morphology off-chip. More importantly, when mEFs were fused to mESCs in our microfluidic device and plated into a tissue culture dish, we were able to observe reprogramming of mEFs. Because our device maintains cell registration and analysis in the array, we anticipate its use to characterize fusion-mediated reprogramming of somatic cells.

Materials and Methods

Microfluidic device fabrication and setup

Masters for the microfluidic device were made from SU8 (MicroChem) spun on silicon wafers using standard photolithographic techniques[29] (Supplementary Figs. 1 and 10 online show dimensions and masks). PDMS was poured over the master and then degassed before curing. Glass slides with electrodes were constructed from mask blanks pre-coated with chrome and photoresist (Telic), patterned by a transparency mask exposed to UV. The PDMS devices and glass slides were assembled using plasma bonding.

The devices were blocked with 7.5% bovine serum albumin and rinsed with phosphate-buffered saline before use. Cells were manually placed in the top inlet reservoir and drawn through the device at 15–50 μm/s using a syringe pump.

PEG Fusion in the Microfluidic Device

5×10^5 cells of each cell type were pelleted and resuspended in ~500 μL of media, filtered through a 35 μm cell strainer (BD Falcon), and loaded into the device as described previously. PEG-1500 was put into the inlet reservoir and drawn past the cells at 0.4 μL/min for 3–5 min. The cells were washed with warm 1:1 PEG:media for 1 min, then incubated in warm media for 26 min. At t = 30 min, the cells were washed with trypan blue (10% in PBS) for 5 min, then with media for 5 min. At t = 40 min the second dose of PEG was applied, and the entire protocol was repeated for a total of 4 doses

Electrofusion in the Microfluidic Device

We connected the electrodes to a power supply (Eppendorf) in parallel with a 50 kΩ resistor . After cell loading, we flushed with hypoosmolar fusion buffer at 0.4 μL/min for 10 min. The cells were pulsed at varying voltages (0.5 to 2.0 kV/cm) for 50 μs × 5 pulses. Hypoosmolar fusion buffer was flushed past the cells for an additional 10 min before being replaced with warm media. The cells were then incubated for an additional 15 min at 37 °C.

Image Acquisition and Analysis

The microfluidic device was placed on an automated inverted microscope (Zeiss Axiovert 200m) fitted with a stage incubator (In Vivo Scientific) and images were acquired either every 2.5 min or 5 min. A single randomly chosen image field (~200–300 capture combs) was used for each experiment, and the size of the image field remained constant. Images were analyzed in ImageJ (http://rsb.info.nih.gov/ij/) to determine pairing efficiencies (number of traps in the field of view occupied with a single cell of one type in the bottom of the well with a second cell (or more) of the other type on top) and fusion efficiencies (based on fluorescence exchange or membrane reorganization). Fluorescence exchange efficiencies were also analyzed using an automated macro written in ImageJ.

See Supplementary Methods online for full fabrication, assembly, fusion, and imaging details.

Supplementary Material

Refer to Web version on PubMed Central for supplementary material.

Acknowledgments

This research was supported by the National Aeronautics and Space Administration and the National Institutes of Health (EB007278 and EB008550 to JV and 5-R37CA084198 and 5-R01-HDO45022 to RJ). All microfluidic devices were constructed in the Microsystems Technology Laboratory at MIT. The authors wish to thank S. Desai (MIT) for the eGFP and DsRed mouse 3T3 fibroblasts and to R. Foreman (MIT) for Oct4-GFP MEFs. We are very thankful to N. Kunst (Fraunhofer Institute) and T. van Boxtel (MIT) for fruitful discussions.

References

1. Blau HM, Pavlath GK, Hardeman EC, Chiu CP, Silberstein L, Webster SG, Miller SC, Webster C. Plasticity of the Differentiated State. Science. 1985; 230:758. [PubMed: 2414846]
2. Kohler G, Milstein C. Continuous Cultures of Fused Cells Secreting Antibody of Predefined Specificity. Nature. 1975; 256:495. [PubMed: 1172191]
3. Miller RA, Ruddle FH. Pluripotent Teratocarcinoma-Thymus Somatic-Cell Hybrids. Cell. 1976; 9:45. [PubMed: 61820]
4. Tada M, Tada T, Lefebvre L, Barton SC, Surani MA. Embryonic germ cells induce epigenetic reprogramming of somatic nucleus in hybrid cells. Embo J. 1997; 16:6510. [PubMed: 9351832]
5. Wilmut I, Schnieke AE, McWhir J, Kind AJ, Campbell KHS. Viable offspring derived from fetal and adult mammalian cells. Nature. 1997; 385:810. [PubMed: 9039911]
6. Matveeva NM, Shilov AG, Kaftanovskaya EM, Maximovsky LP, Zhelezova AI, Golubitsa AN, Bayborodin SI, Fokina MM, Serov OL. In vitro and in vivo study of pluripotency in intraspecific hybrid cells obtained by fusion of murine embryonic stem cells with splenocytes. Molecular Reproduction And Development. 1998; 50:128. [PubMed: 9590528]
7. Tada M, Takahama Y, Abe K, Nakatsuji N, Tada T. Nuclear reprogramming of somatic cells by in vitro hybridization with ES cells. Current Biology. 2001; 11:1553. [PubMed: 11591326]
8. Flasza M, Shering AF, Smith K, Andrews PW, Talley P, Johnson PA. Reprogramming in inter-species embryonal carcinoma-somatic cell hybrids induces expression of pluripotency and differentiation markers. Cloning Stem Cells. 2003; 5:339. [PubMed: 14733752]
9. Jahn R, Lang T, Sudhof TC. Membrane fusion. Cell. 2003; 112:519. [PubMed: 12600315]
10. Pontecorvo G. Production of Mammalian Somatic-Cell Hybrids by Means of Polyethylene-Glycol Treatment. Somat Cell Genet. 1975; 1:397. [PubMed: 1242069]
11. Davidson RL, Gerald PS. Improved Techniques for Induction of Mammalian-Cell Hybridization by Polyethylene-Glycol. Somat Cell Genet. 1976; 2:165. [PubMed: 1028164]
12. Vienken J, Zimmermann U. Electric Field-Induced Fusion -Electrohydraulic Procedure for Production of Heterokaryon Cells in High-Yield. Febs Lett. 1982; 137:11. [PubMed: 7067814]
13. Zimmermann U, Vienken J. Electric Field-Induced Cell-to-Cell Fusion. J Membrane Biol. 1982; 67:165. [PubMed: 7050391]
14. Stromberg A, Ryttsen F, Chiu DT, Davidson M, Eriksson PS, Wilson CF, Orwar O, Zare RN. Manipulating the genetic identity and biochemical surface properties of individual cells with electric-field-induced fusion. Proc Natl Acad Sci USA. 2000; 97:7. [PubMed: 10618361]
15. Tresset G, Iliescu C. Electrical control of loaded biomimetic femtoliter vesicles in microfluidic system. Applied Physics Letters. 2007; 90:173901.
16. Tresset G, Takeuchi S. A microfluidic device for electrofusion of biological vesicles. Biomedical Microdevices. 2004; 6:213. [PubMed: 15377830]
17. Schut TCB, Kraan YM, Barlag W, Deleij L, Degrooth BG, Greve J. Selective Electrofusion of Conjugated Cells in Flow. Biophysical Journal. 1993; 65:568. [PubMed: 8218887]
18. Wang J, Lu C. Microfluidic cell fusion under continuous direct current voltage. Applied Physics Letters. 2006; 89:234102.
19. Khine M, Lau A, Ionescu-Zanetti C, Seo J, Lee LP. A single cell electroporation chip. Lab on a Chip. 2005; 5:38. [PubMed: 15616738]
20. Lee PJ, Hung PJ, Shaw R, Jan L, Lee LP. Microfluidic application-specific integrated device for monitoring direct cell-cell communication via gap junctions between individual cell pairs. Applied Physics Letters. 2005; 86
21. Khine M, Ionescu-Zanetti C, Blatz A, Wang LP, Lee LP. Single-cell electroporation arrays with real-time monitoring and feedback control. Lab On A Chip. 2007; 7:457. [PubMed: 17389961]
22. Valero A, Post JN, Nieuwkasteele JWv, Braak PMt, Kruijer W, Berg Avd. Gene transfer and protein dynamics in ste cells using single cell electroporation in a microfluidic device. Lab on a Chip. 2007; 8:62. [PubMed: 18094762]

23. Di Carlo D, Aghdam N, Lee LP. Single-cell enzyme concentrations, kinetics, and inhibition analysis using high-density hydrodynamic cell isolation arrays. Anal Chem. 2006; 78:4925. [PubMed: 16841912]
24. Sowers AE. Characterization of Electric Field-Induced Fusion in Erythrocyte Ghost Membranes. J Cell Biol. 1984; 99:1989. [PubMed: 6438112]
25. Silva J, Chambers I, Pollard S, Smith A. Nanog promotes transfer of pluripotency after cell fusion. Nature. 2006; 441:997. [PubMed: 16791199]
26. Wong CC, Gaspar-Maia A, Ramalho-Santos M, Reijo Pera RA. High-efficiency stem cell fusion-mediated assay reveals Sall4 as an enhancer of reprogramming. PLoS ONE. 2008; 3:e1955. [PubMed: 18414659]
27. Wernig M, Meissner A, Foreman R, Brambrink T, Ku MC, Hochedlinger K, Bernstein BE, Jaenisch R. In vitro reprogramming of fibroblasts into a pluripotent ES-cell-like state. Nature. 2007; 448:318. [PubMed: 17554336]
28. Takahashi K, Yamanaka S. Induction of pluripotent stem cells from mouse embryonic and adult fibroblast cultures by defined factors. Cell. 2006; 126:663. [PubMed: 16904174]
29. Rosenthal A, Macdonald A, Voldman J. Cell patterning chip for controlling the stem cell microenvironment. Biomaterials. 2007; 28:3208. [PubMed: 17434582]

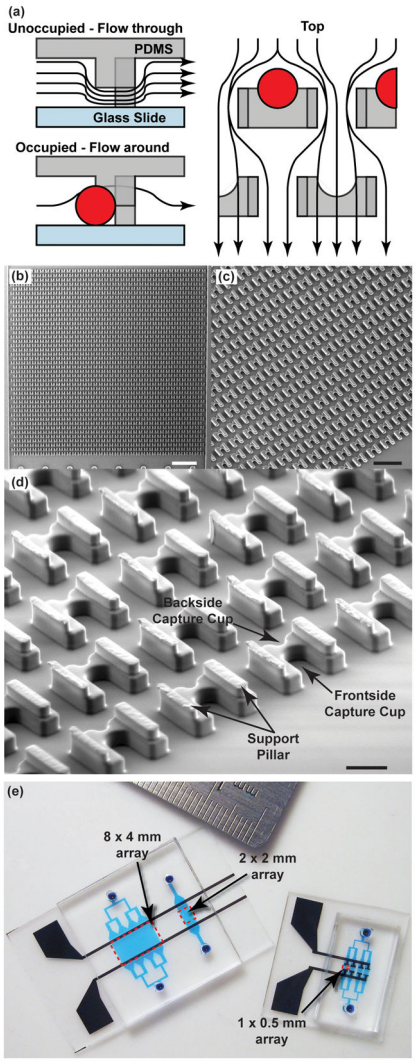

Figure 1.

Microfluidic device for cell capture and pairing. (**a**) Schematic of the microfluidic device operation and structure. The flow passes underneath the cell trap, directing the cells into the capture cup. The support pillars maintain the proper vertical gap. (**b–d**) Scanning electron micrograph images of the PDMS device at various magnifications. **(b)** Overview of the 2 mm × 2 mm device, which contains 1166 cell traps; scale bar, 250 μm. (**c**) Close-up image showing the densely packed structures; scale bar, 100 μm. (**d**) Detail of the trap structure, including the larger frontside and smaller backside capture cups (14 μm tall, 18 μm wide x 25–40 μm deep and 10 μm wide x 5 μm deep, respectively), along with support pillars (7.5 μm wide x 35–50 μm long x 6 to 8 μm tall); scale bar, 20 μm. (**e**) Images of the three device geometries. The 2 x 2 mm array is in a 1.8-cm-long channel and contains ~750 to 1200 traps, the 8 x 4 mm array is in a 2.5-cm-long device and contains ~ 6000 traps, and the 1-mm-wide x 0.5-mm-long array (used primarily for optimization of trap geometry and fusion voltages) is in a 1.8-cm-long device array and contains ~ 100 traps per channel.

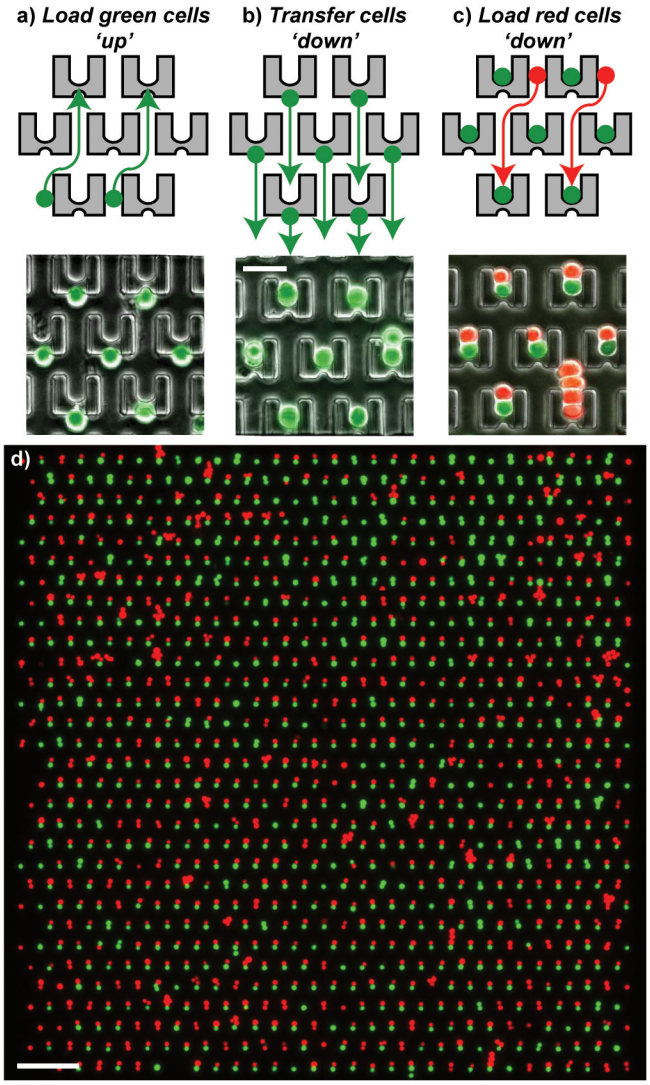

Figure 2.

Three-step cell loading protocol. (**a**) Cells are first loaded “up” towards the smaller backside capture cup. (**b**) The direction of the flow is reversed, and the cells are transferred “down” into the larger frontside capture cup 2 rows below; scale bar, 50 μm. (**c**) The second cell type is loaded in from the top, and cells are captured in front of the first cell type. (**d**) Red/green fluorescent overlay image of CellTracker-stained mouse 3T3s loaded into the 2mm x 2mm device. Pairing efficiencies of ~70% are possible with higher efficiencies found in the bottom half of the array; scale bar, 200 μm.

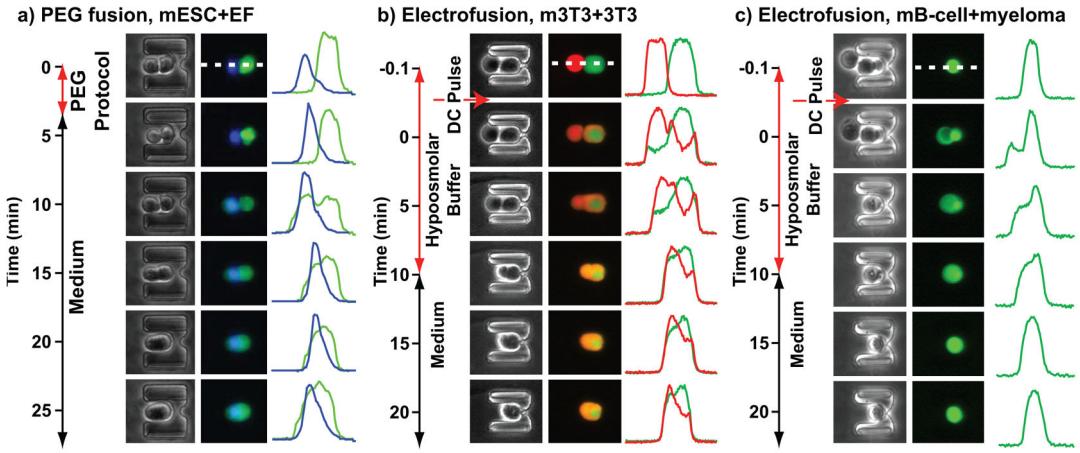

Figure 3.

Timescale of chemical- and electric field-induced fusion for different cell pairs. (**a**) PEG fusion of GFP-expressing mESCs and Hoechst-stained mEFS. Phase images show the status of membrane reorganization while fluorescent overlay images and linescans through the cells demonstrate the exchange of fluorescence. Immediately before and after the PEG dose the fluorescence is sequestered and two cell membranes are distinguishable. At t = 10 min green fluorescence is observed inside the mEF, and at t = 15 min the membranes begin to reorganize. At t = 25 min hybrids are observed that contain the contents of both cells. The mEF nucleus appears to be intact (no fusion with nucleus of mESC). (**b**) Electrofusion of DsRed- and eGFP-expressing mouse 3T3s. Immediately after the fusion pulse exchange of fluorescence is observed, outlining the nuclei of the cells. At t = 10 min the membranes begin to reorganize, and at t = 20 min hybrid cells are observed that contain the contents of both cells. (**c**) Electrofusion of GFP-positive mouse B-cells and unstained myeloma cells. Immediately after the fusion pulse GFP is observed in the properly loaded myeloma cell. The third cell in the comb is not aligned for fusion, therefore no exchange of fluorescence is observed and it falls off after t = 5 min. Membrane reorganization is difficult to observe, but at t = 20 min only one cell membrane is observed.

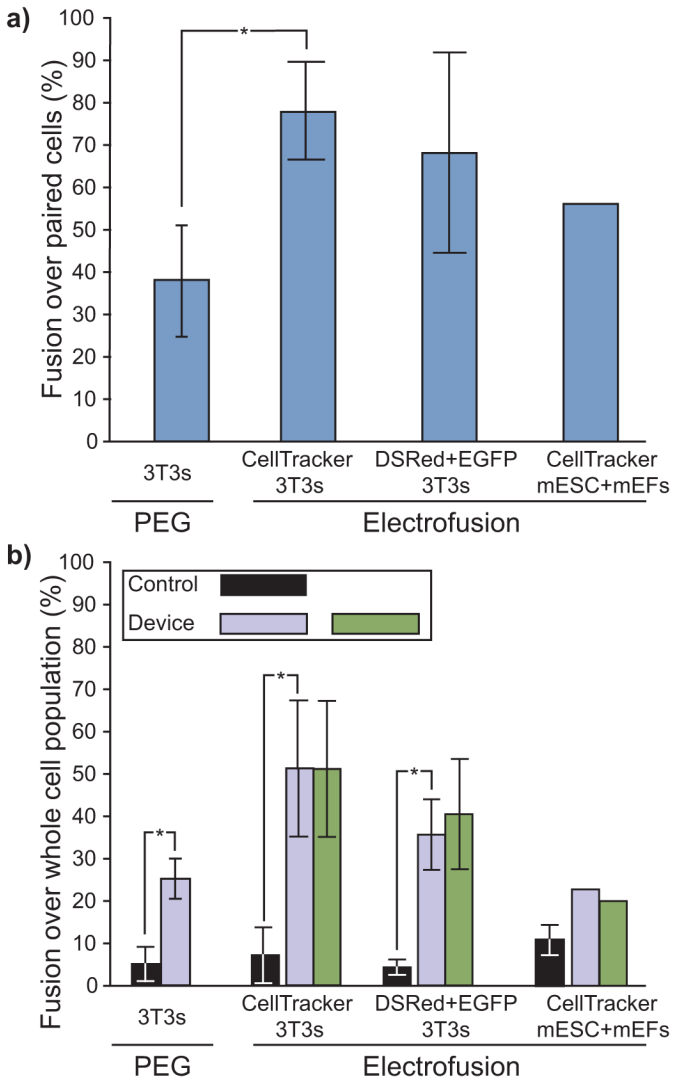

Figure 4.

Comparison of fusion efficiencies. (**a**) Comparison of PEG fusion efficiency using four doses of PEG (see also Supplementary Fig. 2 online) and one dose of electrofusion in the microfluidic device, as determined by visual inspection of the data. Only paired cells were analyzed, allowing a direct comparison of the fusion initiation potential of PEG versus electrofusion. (**b**) Comparison of fusion efficiencies using the microfluidic device and controls. The values are based on red-green double-positive cells across the entire population or device. Both chemical and electrical fusion were analyzed using different cell types. Control values were determined by FACS, while device values were determined by both visual inspection (purple bars) and our image analysis program (green bars). The fusion values determined from the image analysis program agreed within error to those determined through manual inspection. In all cases the device gave a 2-10 fold improvement in fusion efficiency compared to that obtained by the control. Lines with "*" between conditions indicate statistically significant differences by two-sided t-test ($P < 0.05$). Error bars represent standard deviation ($n = 3$ independent trials).

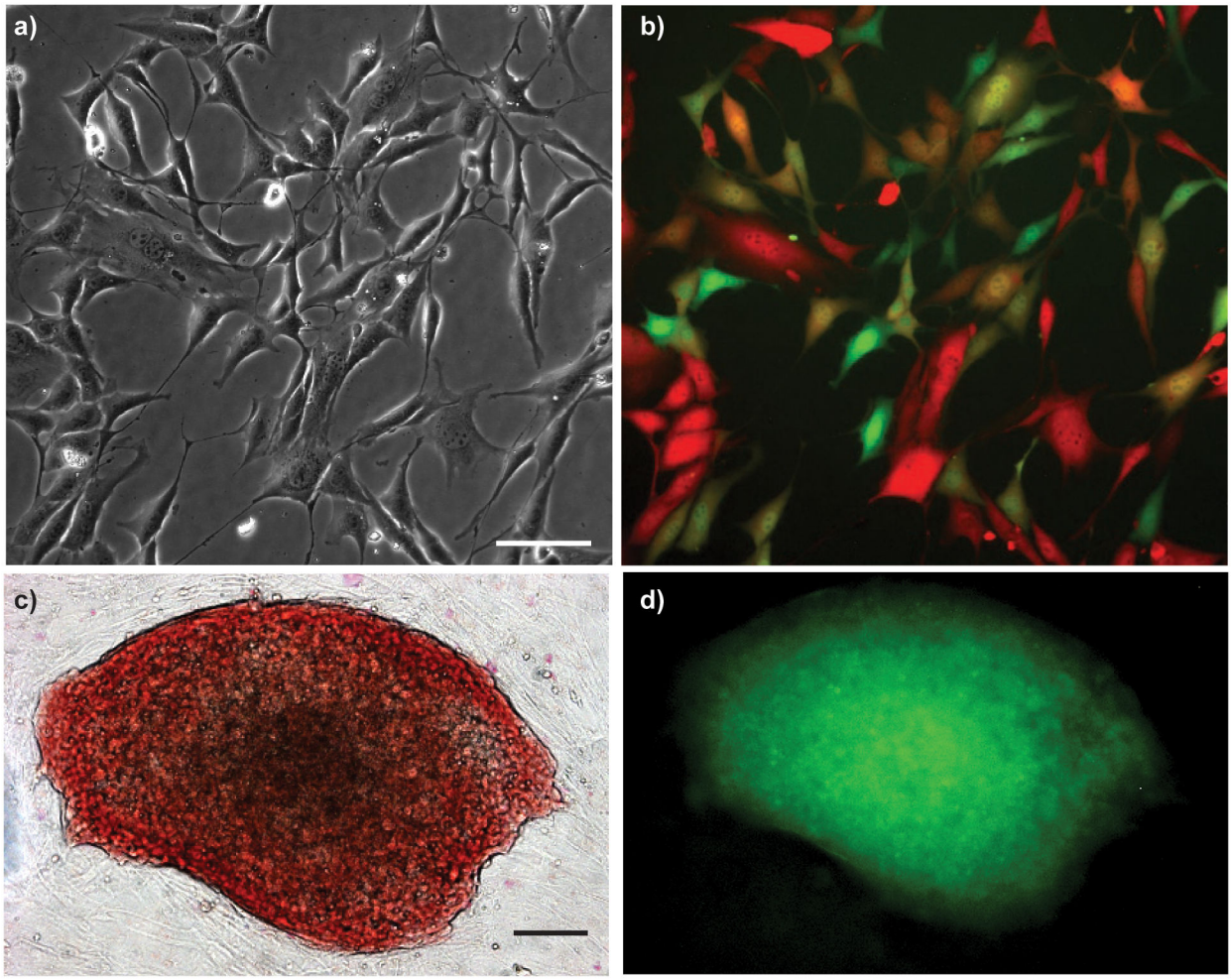

Figure 5.

Functionality of fused cells. (**a**–**b**) Phase and red-green fluorescent image of DSRed/EGFP 3T3s at day 4 after fusion in the microfluidic device indicating the presence of red-green double-positive fused cells; scale bar, 100 μm. (**c–d**) Double-resistant hybrids between Hygromycin B-resistant mESCs and Puromycin-resistant mEFs after fusion in the microfluidic device are viable, have an ESC-like morphology, and stain positive for alkaline phosphatase. Reprogramming of mEFs can be observed, as judged by reactivation of an endogenous Oct4-GFP reporter; scale bar, 100 μm.